

# SURFACE FINISHING OF ADDITIVE MANUFACTURING PARTS FOR PARTICLE ACCELERATORS \*

H. Hähnel<sup>1†</sup>, B. Dedić, Institute of Applied Physics, Goethe University, Frankfurt a. M., Germany  
<sup>1</sup>also at Helmholtz Forschungsakademie Hessen für FAIR (HFHF), Frankfurt a. M., Germany

T. Torims, A. Ratkus, Riga Technical University, Riga, Latvia

M. Vedani, T. Romano, Politecnico di Milano, Italy

M. Vretenar, CERN, Geneva, Switzerland

M. Pozzi, Rösler Italian S.R.L, Concorezzo, Italy

E. Chyhyrynets, R. Caforio, C. Pira, INFN Laboratori Nazionali di Legnaro, Legnaro (PD), Italy

N. Kunkel, Technische Hochschule Mittelhessen (THM), Friedberg, Germany

## Abstract

Significant progress towards the suitability of Additive Manufacturing (AM) metal parts for the production of linear accelerator components has been made in recent years. One significant factor for the suitability of AM parts to produce linac rf structures is the surface quality of the parts. Due to the inherently higher surface roughness of AM metal parts, post-processing is necessary to reach surfaces suitable for rf operation. We present most recent results of surface post-processing trials with AM parts from stainless steel.

## INTRODUCTION

Additive manufacturing (AM) of stainless steel and pure copper parts for the manufacturing of critical parts for linear particle accelerators is an interesting prospect for cost reduction of these typically very complex structures [1–9]. First implementations of stainless steel parts use an oversize print that is CNC machined and then copper plated with the rest of the linac cavity [10–12]. The main benefit there is the inclusion of complex cooling channels within the parts. These implementations therefore still need very costly and time consuming machining of the surface to achieve the dimensional accuracy and surface roughness needed. However, to fully harness the potential cost savings of metal AM, this step should be eliminated. To reach this goal, we need to identify surface finishing (polishing) processes, that can produce parts with low surface roughness ( $R_a < 1 \mu\text{m}$ ) while maintaining the dimensional accuracy of the part or at least show predictable mass removal of the part geometry.

In this paper, we summarize the current state of a study to try to answer these questions for steel AM parts. To this end, a small, cheap to print test geometry was developed to evaluate as many geometrical scenarios as possible to differentiate the different processes tested (see Fig. 1).

\* Work supported by: BMBF 05P21RFRB2.

This project has received funding from the European Union's Horizon 2020 Research and Innovation programme under grant agreement No 101004730 and is supported by the Latvian Council of Science under grant agreement VPP-IZM-CERN-2022/1-0001.

Development of PEP technology financed from: PNRR MUR project PE0000023-NQSTI.

<sup>†</sup> haehnel@iap.uni-frankfurt.de

## TEST GEOMETRIES

The aforementioned test geometry is shown in Fig. 2, where the purpose of the different features is noted. In addition to different simple geometric features to stress test surface finishing techniques, a short stem with a modified drift tube structure from an IH-DTL is positioned on top of the part for evaluation of a more realistic scenario as found in linac structures [3]. The test part measures 61 mm×20 mm×55 mm and is therefore more cost-effective than printing full large linac geometries just for testing.

At this time, a total of 12 of these test samples have been printed at the company Rosswag (samples 1–5) as well as by colleagues at THM Friedberg with a focus on high part accuracy (samples 6–12), as shown in Fig. 1. While samples 9–12 were not sandblasted (SB) after printing (see Fig. 3), all other parts were sandblasted after printing to remove residual powder from the parts surface.

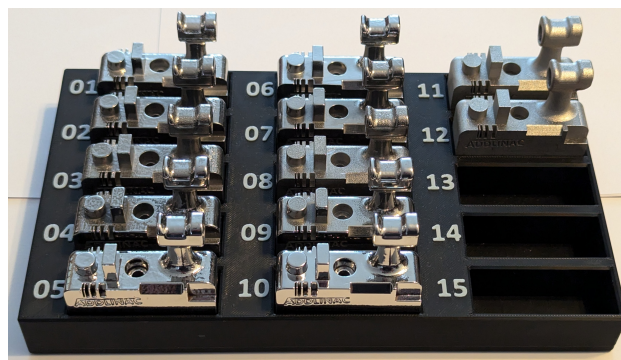


Figure 1: Test geometries in sorting rack. Samples 11 and 12 are still unprocessed.

## SURFACE FINISHING PROCESSES

Test samples were sent to different companies and researchers for surface finishing with different techniques. The processes used for this study so far are summarized in Table 1. The processes include two trials with vibratory mass finishing (PERS, Rösler), which is known to be able to produce very smooth parts at higher processing times. One potential

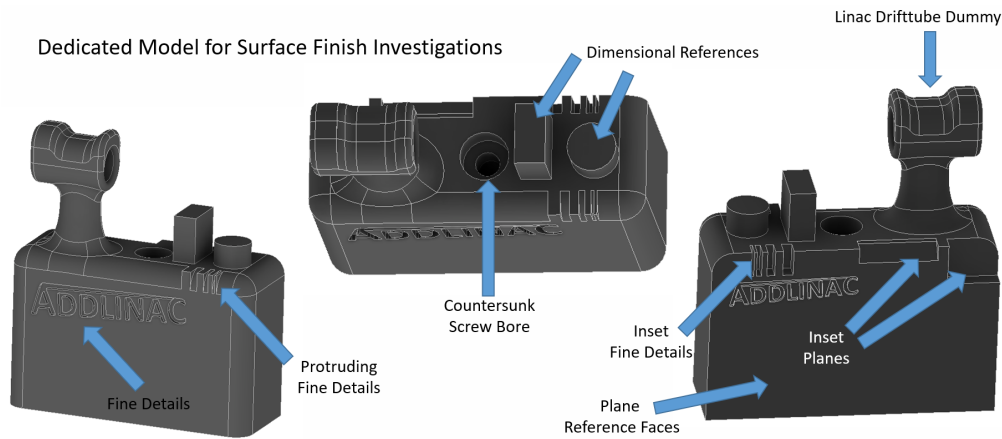


Figure 2: Test geometry for dedicated surface finishing studies. The individual features are noted on the picture. Longest side of the part is 61 mm.

drawback is the rounding of hard edges which increases with process time. Another trial was done with a combination of wet sandblasting for preprocessing and a finishing using a dry electrolytic method called DLyte. While wet sandblasting can lead to significant non-uniform mass removal, the DLyte process can produce very low surface roughness. Finally, two samples were processed using plasma electrolytic polishing (PEP), which can be considered to be a more environmentally friendly alternative to electrochemical polishing due to the use of relatively harmless solutions during the process. Additionally, PEP in contrast to other chemical or electrochemical processes is capable of reducing roughness by an order of magnitude without the need of a mechanical pre-treatment at much shorter process times [13].

Table 1: Description of Surface Finishing Processes

Process Name	Process Description
Spaleck	linear high frequency processing PPL300, fixed sample, 5.5h
WB+DLyte	1. wet sand blasting 2. DLyte polishing
PERS	vibratory mass finishing 4h VL150B + 2h VT145
Rösler	vibratory mass finishing three step process (total 48h)
INFN, PEP	plasma electrolytic polishing 130 to 150 min, 300V, 90°C

## SURFACE FINISHING RESULTS

A full summary of the measured surface roughness numbers after the different surface finishing processes is given in Table 2. After printing, the initial surface roughness for Rossowag manufactured parts was in the order of  $R_a = 2 \mu\text{m}$  to  $4 \mu\text{m}$ . Parts by THM had an initial roughness of  $R_a = 3 \mu\text{m}$  to  $8 \mu\text{m}$ .

Surface roughness after finishing was measured in two different configurations (“THM” and “Rösler” in Table 2).

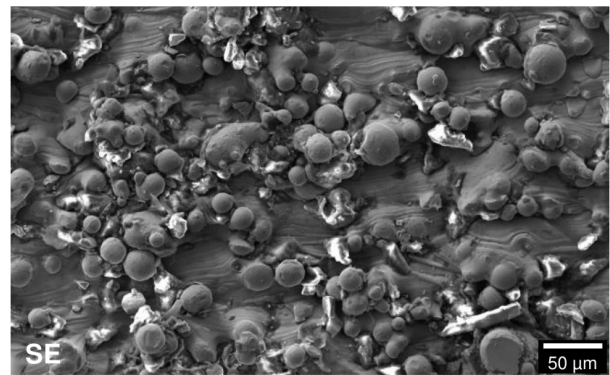


Figure 3: SEM images of the surface for Sample 9 in the unprocessed stage. This sample was not sandblasted after printing (as it would be usually). Therefore, residual powder particles can be seen stuck to the surface. Courtesy of M. Pozzi, Rösler Italy.

The measurements connoted as “THM” were measured using a Keyence Laser Microscope, using a 20x magnification and a cutoff  $\lambda_c = 0.08 \text{ mm}$ .  $R_a$  and  $R_z$  were measured using 10 lines at  $45^\circ$  to the print orientation of the parts.  $S_a$  and  $S_z$  were measured on a  $250 \mu\text{m} \times 250 \mu\text{m}$  area. Measurements at Rösler were performed with a contact profilometer for  $R_a$  and  $R_z$  using five lines with length  $L = 4.8 \text{ mm}$  and a cutoff  $\lambda_c = 0.8 \text{ mm}$  perpendicular and parallel to the printing direction (only values parallel to the print direction are shown, as they show the worst case).  $S_a$  and  $S_z$  were measured using an optical profilometer on a  $1 \text{ mm}^2$  area with a cutoff  $\lambda_c = 0.8 \text{ mm}$ . All surface measurements were performed on the large plane areas on the sides of the test parts. It should be noted, that due to the difference in measurement procedures, the values are not directly comparable.

In addition to the surface roughness measurements, a total of 14 dimensions at the various geometries on the test parts were measured before and after surface finishing to determine the impact on part accuracy imposed by the different methods. These measurements are represented by the mean

Table 2: Surface Roughness and Dimensional Deviations after Surface Finishing

#	Process	Manufacturer	Ra [ $\mu\text{m}$ ]	Rz [ $\mu\text{m}$ ]	Sa [ $\mu\text{m}$ ]	Sz [ $\mu\text{m}$ ]	$\Delta L_{avg}$ [mm]	$\Delta L_{max}$ [mm]	$\sigma_L$ [mm]	Measurement Setup (surf.)
2	(Spaleck)	Rosswag	0.15	0.96	0.18	2.89	0.06	0.13	0.03	THM
7	(Spaleck)	THM	0.21	1.27	0.30	2.98	0.08	0.24	0.06	THM
1	(WB+Dlyte)	Rosswag	0.09	0.58	0.76	7.56	0.37	0.87	0.24	THM
6	(WB+Dlyte)	THM	0.16	1.14	0.82	15.63	0.31	0.87	0.24	THM
3	(PERS)	Rosswag	0.32	2.04	3.24	15.84	0.03	0.11	0.03	THM
8	(PERS)	THM	0.79	4.19	2.46	21.12	0.06	0.21	0.06	THM
4	(Rösler)	Rosswag	0.05	0.50	0.08	3.24	0.03	0.14	0.08	Rösler
9	(Rösler)	THM - no SB	0.03	0.32	0.08	1.36	0.05	0.20	0.06	Rösler
5	(INFN, PEP)	Rosswag	0.25	1.30	0.37	14.02	0.22	0.33	0.10	Rösler
10	(INFN, PEP)	THM - no SB	0.31	3.09	0.40	17.13	0.25	0.38	0.10	Rösler

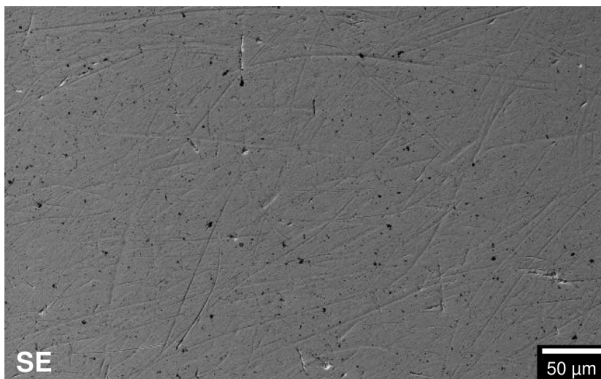


Figure 4: SEM images of the surface for Sample 9 after mass finishing by Rösler. The surface is clearly polished to a high degree. Residual scratch marks from mass finishing can be seen. The surface roughness seen here is  $R_a = 0.03 \mu\text{m}$ . Courtesy of M. Pozzi, Rösler Italy.

deviation  $\Delta L_{avg}$  and the highest single deviation  $\Delta L_{max}$  of all the measured dimensions before and after surface finishing, as well as the standard deviation  $\sigma_L$ .

Looking at the line roughness values in Table 2, all but one part have a roughness of  $R_a \leq 0.5 \mu\text{m}$ . Looking at the surface roughness values  $S_a$  and  $S_z$ , some more distinctions can be made. The overall smoothest surface is produced by Rösler (parts 4 and 9) with the lowest  $S_a$  and  $S_z$  measured (see also Fig. 4). In addition, they also show among the lowest dimensional deviations ( $\Delta L_{avg} = 0.03$  &  $0.05$  mm). It has to be noted, that rounding of hard edges is more pronounced in these parts. Similar performance is observed for the parts processed by Spaleck (parts 2 and 7) using linear high frequency processing. These parts in addition to low surface roughness values, also show a remarkably low geometric deviation of  $\Delta L_{avg} = 0.06$  &  $0.08$  mm, while showing lower edge rounding. The highest dimensional deviation is observed in parts 1 and 6 due to extensive wet blasting before the Dlyte finish. The parts with the lowest geometric deviation are the ones processed by PERS using vibrational mass finishing, but those have by far the highest surface roughness remaining. The parts finished using PEP



Figure 5: Sample 10 after a PEP processing time of 130 minutes.

show relatively high dimensional deviations for this first trial (see Fig. 5).

## CONCLUSION

In conclusion, we have found some interesting candidates for stainless steel surface finishing (e.g. Spaleck, Rösler, PEP) that could be very useful for cost effective production of precise linac components. Dimensional accuracy is an important factor for linac components and has to be considered alongside roughness requirements. Further tests will include copper plating of the test samples followed by cross-sections to determine the layer adhesion. For stainless steel linac parts, the suitability for uniform copper plating is a sufficient criterion to choose a process. When looking towards pure copper AM parts, this may not be sufficient, as the surface conductivity after finishing needs to be considered as well.

## REFERENCES

- [1] T. Romano *et al.*, “Metal Additive Manufacturing for Particle Accelerator Applications”, *Physical Review Accelerators and Beams*, vol. 27, no. 5, p. 054801, 2024.  
doi:10.1103/PhysRevAccelBeams.27.054801
- [2] H. Hähnel, U. Ratzinger, “First 3D Printed IH-Type Linac Structure – Proof-of-Concept for Additive Manufacturing of Linac RF Cavities”, *Instruments*, vol. 6, no. 1, p. 9, 2022.  
doi:10.3390/instruments6010009
- [3] H. Hähnel *et al.*, “Additive Manufacturing of an IH-Type Linac Structure from Stainless Steel and Pure Copper”, *Instruments*, vol. 7, no. 3, p. 22, 2023.  
doi:10.3390/instruments7030022
- [4] H. Hähnel *et al.*, “RF Conditioning of an IH-DTL Cavity Made using Additive Manufacturing”, in *Proc. IPAC’24*, Nashville, TN, USA, May 2024, pp. 3501–3504.  
doi:10.18429/JACoW-IPAC2024-THPR10
- [5] M. Mayerhofer, J. Mitteneder, G. Dollinger, “A 3D Printed Pure Copper Drift Tube Linac Prototype”, *Rev. Sci. Instrum.*, vol. 2, no. 93, p. 023304, 2022.  
doi:10.1063/5.0068494
- [6] M. Mayerhofer *et al.*, “Additive Manufacturing of Side-Coupled Cavity Linac Structures from Pure Copper: A First Concept”, *Instruments*, vol. 7, no. 56, p. 55, 2023.  
doi:10.3390/instruments7040056
- [7] M. Mayerhofer *et al.*, “Improving Fabrication and Performance of Additively Manufactured RF Cavities by Employing Co-Printed Support Structures and Their Subsequent Removal”, *Instruments*, vol. 8, no. 1, p. 18, 2024.  
doi:10.3390/instruments7040056
- [8] M. Mayerhofer *et al.*, “Red and Green Laser Powder Bed Fusion of Pure Copper in Combination with Chemical Post-Processing for RF Cavity Fabrication”, *Instruments*, vol. 8, no. 3, p. 39, 2024.  
doi:10.3390/instruments7040056
- [9] T. Torims *et al.*, “First Proof-of-Concept Prototype of an Additive Manufactured Radio Frequency Quadrupole”, *Instruments*, vol. 5, no. 4, p. 35, 2021.  
doi:10.3390/instruments5040035
- [10] A. Seibel *et al.*, “Welding and Copper Plating Investigations on the FAIR Proton Linac”, in *Proc. LINAC’22*, Liverpool, UK, Aug. 2022, pp. 345–347.  
doi:10.18429/JACoW-LINAC2022-TUPOJ005
- [11] H. Hoeltermann *et al.*, “Technical Design of an IH-type Buncher for KoBRA at RAON”, *J. Korean Phys. Soc.*, vol. 83, pp. 589–594, 2023.  
doi:10.1007/s40042-023-00845-3
- [12] C. Kleffner *et al.*, “Progress and Status of the FAIR Proton Linac”, presented at LINAC’24, Chicago, IL, USA, Aug. 2024, paper TUPB026, this conference.
- [13] E. Chyhrynets *et al.*, “Plasma Electrolytic Polishing Technology Progress Development for Nb and Cu Substrates Preparation”, in *Proc. 21th Int. Conf. RF Supercond. (SRF’23)*, Grand Rapids, MI, USA, Jun. 2023, pp. 75–79.  
doi:10.18429/JACoW-SRF2023-MOPMB009